Available online at www.sciencedirect.com
ScienceDirect
Chinese Journal of Natural Medicines 2019, **17**(7): 0517–0524
Chinese Journal of Natural Medicines

A hepatoprotection study of Radix Bupleuri on acetaminophen-induced liver injury based on CYP450 inhibition

WANG Yu-Xin[1, 3], DU Yi[2], LIU Xia-Fei[2], YANG Fang-Xiu[2], WU Xiao[2], TAN Li[3], LU Yi-Hong[2, 3], ZHANG Jing-Wei[1], ZHOU Fang[1], WANG Guang-Ji[1*]

[1] *Key Lab of Drug Metabolism and Pharmacokinetics, China Pharmaceutical University, Nanjing 210009, China;*
[2] *Key Laboratory of New Drug Research and Clinical Pharmacy, Xuzhou Medical University, Xuzhou 221004, China;*
[3] *Jiangsu Institute for Food and Drug Control, Nanjing 210019, China*

Available online 20 July, 2019

[ABSTRACT] We investigated the potential hepatoprotective effect of Radix Bupleuri (RB) by inducing acute liver injury (ALI) in an animal model using acetaminophen (APAP) after pretreatment with RB aqueous extract for three consecutive days. Compared to those of the APAP group, the biochemical and histological results of the RB pretreatment group showed lower serum aspartate transaminase (AST) and alanine transaminase (ALT) levels as well as less liver damage. Pharmacokinetic study of the toxicity related marker acetaminophen-cysteine (APC) revealed a lower exposure level in rats, suggesting that RB alleviated APAP-induced liver damage by preventing glutathione (GSH) depletion. The results of cocktail approach showed significant inhibition of CYP2E1 and CYP3A activity. Further investigation revealed the increasing of CYP2E1 and CYP3A protein was significantly inhibited in pretreatment group, while no obvious effect on gene expression was found. Therefore, this study clearly demonstrates that RB exhibited significant protective action against APAP-induced acute live injury *via* pretreatment, and which is partly through inhibiting the increase of activity and translation of cytochrome P450 enzymes, rather than gene transcription.

[KEY WORDS] Hepatoprotection; Radix Bupleuri; Acetaminophen; Acute liver injury; Cytochrome P450 enzymes

[CLC Number] R965 **[Document code]** A **[Article ID]** 2095-6975(2019)07-0517-08

Introduction

Radix Bupleuri (RB) is found in the roots of *Bupleurum chinense* DC. and *B. scorzonerifolium* Willd in herbal medicine [1]. It has been widely used for clearing heat, relieving exterior syndrome, regulating the liver-qi, and lifting yang-qi [2]. With the development of pharmacology and molecular biology, it has been revealed that RB possesses many other valuable properties, one of which is hepatoprotection [3]. RB polysaccharides are reported to exhibit a hepatoprotective effect by analysing aspartate transaminase (AST), alanine transaminase (ALT), and alkaline phosphatase (ALP) activities in mice [4], and complement activation *via* both the classical and alternative pathways was also inhibited [5]. RB essential oils were found to have strong antimicrobial and antifungal activities [6-7]. Additionally, RB lignans also exhibits hepatoprotective activity [8-10]. The traditional preparation of RB, such as Zheng-Chai-Hu-Yin Particles (a Chinese herbal compound containing RB, sileris, tangerine peel, paeoniae, licorice, and ginger) and Xiao Chai Hu Particles (a Chinese herbal compound containing RB, scutellaria, pinellia, dang shen, ginger, licorice, and jujube), are often used or even combined with acetaminophen (APAP) to offered symptomatic relief for patients in clinic suffering from fever, inflammation and influenza [11]. Therefore, in the present study, we aimed to investigate whether APAP-induced acute hepatic toxicity will be alleviated if APAP is coupled with RB.

APAP is a widely used analgesic antipyretic agent worldwide, and will cause acute hepatic necrosis at higher doses [12], the use of which is limited and monitored by government agencies such as the FDA and the CMS [13]. APAP-induced hepatotoxicity is mainly caused by *N*-acetylbenzoquinoneimine (NAPQI), a cytochrome P450-mediated metabolite, which normally conjugates with glutathione to detoxify, then further yields acetaminophen-cysteine (APC) and acetamino-

[Received on] 09-Apr.-2019
[Research funding] This work was supported by State Project for Essential Drug Research and Development of China (No. 20152X09303001).
[*Corresponding author] E-mail: guangjiwang@hotmail.com
These authors have no conflict of interest to declare.

phen-mercapturate (APM) [14]. Excessive dosage of APAP leads to overproduction of NAPQI, which then binds to cellular proteins and causes hepatic necrosis and liver damage after depleting hepatic glutathione (GSH) [15]. Any drug or therapeutic intervention that reduces the formation of NAPQI will therefore help to protect the liver from toxicity.

This hepatotoxic metabolite of APAP is mainly produced by cytochrome P450 enzymes (CYP450), a superfamily of hemoproteins that catalyzes the oxidative metabolism of many exogenous chemicals and endogenous compounds [16]. The CYP enzymes, namely CYP2E1, CYP1A2, and CYP3A4, are primarily responsible for APAP bioactivation that promotes hepatotoxicity in the human liver [17-19]. A compound that inhibits one or more of the CYP450 enzymes listed above may contribute to reduction of hepatotoxicity. To uncover the effects and underlying mechanisms of RB against APAP-induced acute liver injury, a "cocktail" approach was used to monitor its influences on CYP450 activation. Furthermore, mRNA expression and protein expression levels of CYP450 enzymes were measured using western blots and real-time polymerase chain reactions (Real-Time PCR), respectively.

Materials and Methods

Chemicals and regents

Dextromethorphan (DXM, purity ≥ 98.0%, S-1390613), midazolam (MDZ, purity ≥ 98.0%, D01-20141103), tolbutamide (TBM, purity ≥ 98.0%, 017K1025), omeprazole (OME, purity ≥ 96.0%, 9XTF-8N37), chlorzoxazone (CZX, purity ≥ 98.0%, 41M0025V) , dextrorphan (DXO, purity ≥ 98.0%, 10-MAR-15-01), 1-hydroxymidazolam (1-MDZ, purity ≥ 98.0%, UC431), 4-hydroxytolbutamide (4-TBM, purity ≥ 98.0%, 483-138-1V), 5-hydroxyomeprazole (5-OME, purity ≥ 95.0%, BCBQ2933V), 6-hydroxychlorazole (6-CZX, purity, 1385519V) and theophylline (purity ≥ 99.0%, YJX6-F86M) were all from Sigma-Aldrich Chemical Co., Ltd. (St. Louis, MO, USA). 3-Cysteinylacetaminophen trifluoroacetic acid salt (APC, purity ≥ 99.0%, 1-PQY-180-1) was purchased from the Toronto Research Chemicals Co., Ltd. (Toronto, Canada). Internal standard diazepam (DZP, purity ≥ 98.0%, 171220-200903) were received from the National Institute for the Control of Pharmaceutical and Biological Products (Beijing, China). Acetaminophen (APAP, purity ≥ 99.0%, D1513003) was purchased from Shanghai Aladdin Bio-Chem Technology Co., Ltd. (Shanghai, China). HPLC-grade acetonitrile and methanol were purchased from Merck (Merck Company, Darmstadt, Germany). Other chemicals and reagents were of analytical grade. The solid-phase cartridge was from Waters Chromatography (Oasis HLB 3 cc, Milford, MA, USA). Deionized water was purified using the Milli-Q system (Millipore, Milford, MA, USA).

The aqueous extract of RB (Batch #20140305) was supplied by Nantong Jinghua Pharmaceutical Co., Ltd. (Jiangsu, China). The aqueous extract from powdered RB (380 g) was extracted by mixing powdered RB with water and heating for 90 min, twice. The two collections of aqueous extract were combined and concentrated to about 100 mL.

Experimental animals and treatment

Male ICR mice (18–20 g) were purchased from the Beijing Vital River Laboratory Animal Technology Co., Ltd., Nanjing Branch, Nanjing, China [SCXK (su) 2016-0003]. Male Wistar rats (180–200 g) were purchased from the Beijing Vital River Laboratory Animal Technology Co., Ltd., Beijng, China [SCXK (jing) 2016-0006]. Before the experiment, the rats were allowed a 1-week acclimation period with free access to standard rodent chow and water under controlled conditions (2 h light-dark cycle at 23 ± 1 °C, 55% ± 5% humidity). Regulations of Experimental Animal Administration issued by the Ministry of Science and Technology of the People's Republic of China (http: //www.most.gov.cn) were followed, and animal protocols were approved by the Ethics Committee for the Care and Use of Laboratory Animals at China Pharmaceutical University (Jiangsu, China).

Because mice are more sensitive to APAP-induced liver injury then rats, biochemical and histological studies were conducted using ICR mice first. Mice were randomly divided into six groups containing six mice each: (1) Vehicle (saline); (2) APAP (0.5 g·kg^{-1}); (3) RB low dosage (RBL, 9 g·kg^{-1} RB); (4) RB high dosage (RBH, 36 g·kg^{-1} RB); (5) RBL (9 g·kg^{-1} RB) + APAP (0.5 g·kg^{-1}); (6) RBH (36 g·kg^{-1} RB) + APAP (0.5 g·kg^{-1}). Rats were used to further the pharmaceutical and molecular biological investigation, and were randomly divided into 9 groups of six rats each: (1) Vehicle (saline); (2) APAP (1.2 g·kg^{-1}); (3) Rifampicin (RFP, 50 mg·kg^{-1}); (4) Ketoconazole (KCZ, 80 mg·kg^{-1}); (5) Disulfiram (DSF, 40 mg·kg^{-1}); (6) RB low dosage (RBL, 6 g·kg^{-1} RB); (7) RB high dosage (RBH, 25 g·kg^{-1} RB); (8) RBL (6 g·kg^{-1} RB) + APAP (1.2 g·kg^{-1}); (9) RBH (25 g·kg^{-1} RB) + APAP (1.2 g·kg^{-1}). Each group was administered the assigned drug for three consecutive days, while the APAP group was administered the vehicle. Approximately 6h after the third dose, APAP was administered orally in the APAP and combination groups, while others were administered 5% sodium carboxymethyl cellulose (CMC-Na, the vehicle of APAP) and were killed 24h. microsomes were prepared by calcium precipitation at low temperature, and the protein concentration of the microsomes was determined by bicinchoninic acid (BCA) protein quantification.

Biochemical and histological assessment

The concentrations of ALT and AST in serum were detected using an automatic biochemical analyzer (Siemens, Germany). Liver tissue was fixed in 10% formalin, then embedded in paraffin, cut into sections, and stained with hematoxylin and eosin. After imaging using an optical microscope, the necrosis and degeneration areas of the images were compared using semi-quantitative analyses and Image-Pro Plus 6.0 software (Media Cybernetics, Rockville, MD, USA).

LC-MS/MS analysis of toxicity biomarkers

To study the formation of the hepatotoxic metabolite NAPQI, its subsequent metabolite, acetaminophen-cysteine (APC), was quantified using a Finnigan Surveyor HPLC system (Thermo Electron, San Jose, CA, USA). A Waters XBridge HSS T3 column (2.1 mm × 150 mm, 3.5 μm) was used for separation, with column and autosampler tray temperatures at 35 °C and 4 °C, respectively. Samples were eluted with respectively A (0.1 % formic acid in water) and B (acetonitrile) at a flow rate of 0.2 mL·min^{-1}, with a gradient elution: a linear increase from 2% to 30% in the first 12 min, followed by 30% to 90% for the next 1 min, then returned to 2% B and maintained for the last 3 min. The injection volume was 5 μL.

The mass spectrometer was a Finnigan TSQ Quantum Discovery MAX system (Thermo Electron, San Jose, CA, USA). Data acquisition was performed with Xcalibur 1.2 software (Thermo Finnigan, USA). Peak integration and calibration were performed using LCQUAN software (Thermo Finnigan, USA). The optimized MS conditions were as follows: for the ESI source, capillary temperature and capillary voltage were 350 °C and 3800 V, respectively, while gas pressure and auxiliary airflow were 35 psi and 5 arb, respectively. Quantification was performed using selective reaction monitoring (SRM) of the transition from *m/z* 271.1→182.1 for APC and 180.9→124.2 for theophylline (IS), with a scan time of 0.2 s per transition. The collision energies for APC and IS were 14 and 18 eV, respectively.

Starting with a 100 μL plasma sample, 300 μL precipitant (0.1% formic acid in a mixture of 50% methanol and 50% acetonitrile) was added and the mixture was vortexed for 3 min in a 1.5 mL polypropylene tube, then centrifuged at 18 000 r·min^{-1} for 10 min. 200 μL of the supernatant was taken and evaporated. The residuals were dissolved in 200 μL of the mobile phase, vortexed for 3 min , centrifuged again for 5 min, and then measured with LC/MS/MS.

Measurement of liver CYP activity

CYP2D6, CYP2C9, CYP2E1, CYP2C19, and CYP3A1 (a homolog of CYP3A4 in human) all play an important role in the formation of NAPQI. The activation of each CYP was determined using LC-MS/MS based on a cocktail incubation approach, western blots and PCR analysis. The incubation mixture had a total volume of 200 μL and contained 0.5 mg·mL^{-1} rat microsomal proteins as well as CYP probe substrates (5 μmol·L^{-1} CZX for CYP2E1, 7.5 μmol·L^{-1} DXM for CYP2D, 12.5 μmol·L^{-1} TBM and 5 μmol·L^{-1} OME for CYP2C, 1.25 μmol·L^{-1} MDZ for CYP3A). This initial mixture was preincubated for 5 min at 37 °C. The reaction was initiated by the addition of 1.25 mmol·L^{-1} NADPH and terminated after 30 min with 200 μL ice-cold acetonitrile (including 10 μmol·L^{-1} diazepam as internal standard). All samples were stored at −80 °C immediately after collection.

The incubation mixture was thus prepared, and the metabolites (6-hydroxychlorazole (6-CZX), dextrorphan (DXO), 4-hydroxytolbutamide (4-TBM), 1-hydroxymidazolam (1-MDZ), and 5-hydroxyomeprazole (5-OME)) of these CYP probe substrates in all samples were analyzed using LC-MS/MS.

Sample preparation for LC-MS/MS analysis

Solid phase extraction (SPE) was used to extract the metabolites of cocktail probe substrates from the incubation samples. SPE cartridges were previously activated with 1 mL methanol and equilibrated with 1 mL water. Thereafter, 350 μL samples were thawed in a water bath at 37 °C then added onto the cartridge. The elution was then evaporated under an air stream at 40 °C and the residue was reconstituted with 55% methanol (*V/V* in water) to a volume of 350 μL. After centrifugation, 5 μL of each sample was injected into the LC-MS/MS.

LC-MS/MS analysis of cocktail probe substrates

The metabolites of cocktail probe substrates were simultaneously identified on a Finnigan Surveyor HPLC system (Thermo Electron, San Jose, CA, USA). Separations of analysis were achieved using a Waters XBridge CSH C_{18} column (2.1 mm × 150 mm, 3.5 μm). The column and autosampler tray temperatures were set at 35 and 4 °C, respectively. Samples were eluted with solution A (0.1% formic acid in water) and solution B (0.1% formic acid in methanol) at a flow rate of 0.2 mL·min^{-1} with a gradient elution: an isocratic elution of 55% B for the first 5 min, followed by 88% B from 5.01 to 9 min, then a return to starting conditions for the next 3 min. The injection volume was 5 μL.

The mass spectrometer was a Finnigan TSQ Quantum Discovery Max system (Thermo Electron, San Jose, CA, USA). Data acquisition was performed with Xcalibur 1.2 software (Thermo Finnigan, USA). Peak integration and calibration were performed using LCQUAN software (Thermo Finnigan, USA). The optimized MS conditions were as follows: for the ESI source, capillary temperature and capillary voltage were 350 °C and 3800 V, respectively, while gas pressure and auxiliary airflow were 35 psi and 5 arb, respectively. Analyte- and IS-specific MRM transitions, ESI mode, and collision energy are provided in Table 1.

Table 1 Analyte- and IS-specific ESI-MS/MS parameters

Compound	ESI mode	MRM transition (precursor→product *m/z*)	Collision energy (ev)
6-CZX	–	184.00→120.00	20
DXO	+	258.05→157.22	38
4-TBM	+	287.00→171.00	17
1-MID	+	342.04→203.12	26
5-OME	+	362.00→214.00	12
DZP	+	285.10→193.10	31

Western blot analysis

For western blot analysis of protein expression, livers were washed twice with ice-cold PBS and homogenized in RIPA Lysis Buffer. Supernatants were collected after centrifugation at 14 000 × *g* at 4 °C for 10 min. Protein concentrations were quantified using the BCA method (Pierce

Chemical) [20]. After heat-denaturation, 50 μg of each protein sample was loaded for separation on an SDS nuPAGE Bis-Tris gel (Invitrogen, Carlsbad, California, USA), and then transferred onto poly vinylidene fluoride (PVDF) membranes. Membranes were blocked in 5% BSA blocking reagent for 40 min at 37 °C, followed by primary antibody (for CYP3A and CYP2E1) treatment and incubation at 37 °C for 90 min, then 4 °C overnight. The membranes were washed with TBS buffer three times and then incubated with goat anti-mouse antibody for 90 min at 37 °C. The bound secondary antibody was captured using a gel imaging analysis system (Tanon Science & Technology Co., Ltd., Shanghai, China). The housekeeping protein *β*-actin was used as a loading control. The difference in gray intensity between CYPs and the control protein was calculated using the Image J system (Ver. 1.30v, NIH, USA)

Real Time-PCR assessment

For relative quantitatively analysis of CYP3A and CYP2E1 mRNA levels, 50 mg of rat livers were homogenized with 800 μL TRIzol Reagent (Invitrogen, Carlsbad, California, USA). RNA extraction was performed according to the protocol. RNA quality was evaluated by detecting the 260/280 ratio (1.8−2.0) with an ultraviolet light spectrophotometer (Shimadzu, Japan). Single-stranded cDNA was synthesized using the iScript cDNA Synthesis Kit (Bio-Rad, USA). Real-Time PCR amplification was performed using the iTaq Universal SYBR Green Supermix (Bio-Rad, USA) in a 10 μL reaction containing 0.4 μL of each primer and 1.5 μL of cDNA. The primers for rat CYP3A (F: 5′-ATCCGAT ATGGAGATCAC-3′, R: 5′-GAAGAAGTCCTTGTCTGC-3′), CYP2E1 (F: 5′-CTCCTCGTCATATCCATCTG-3′, R: 5′-GC AGCCAATCAGAAATGTGG-3′), GAPDH (F: 5′-ATGGTG AGGTCGGTGTGAAC-3′, R: 5′-GTCTTCTGGGTGGCAG TGATG-3′) were designed as reported [21]. The reaction was initiated by heating for 10 min at 95 °C, followed by 40 cycles of the following sequence: 15 s at 95 °C, 30 s at 60 °C, and a final extension step of 30 s at 72 °C. The threshold cycles (C_t) were used to quantify the mRNA expression levels of samples with GAPDH normalization.

Statistical analysis

Data is expressed as mean ± standard deviation (SD). One-way ANOVA followed by an unpaired Student's *t*-test was performed in SPSS 16.0 (IBM Corp., Armonk, NY, USA). *P*-values that were less than 0.05 were considered statistically significant, while those less than 0.01 were considered extremely statistically significant.

Results and Discussion

Biochemical and histological results

After measuring serum hepatic enzyme activities using an automatic biochemical analyzer, significant increases in serum ALT and AST levels were observed in the APAP group compared to the vehicle group. This increase was effectively ameliorated by pretreatment with the aqueous extract of RB (Figs. 1A and 1B). This effect was also shown to be dose-dependent.

Histopathological analysis of H&E-stained liver sections also revealed significant hepatic toxicity after treatment with 0.5 g·kg^{-1} APAP. Several types of pathological damage, such as inflammatory cell infiltration, steatosis, and microvesicular fatty degeneration, were observed in the APAP group, while the structural integrity of nuclei and other organelles remained intact in the in the control group. Treatment with the aqueous extract of RB 3 days before APAP administration, remarkably ameliorated histological hepatic damage. Hepatic necrosis was limited to small, localized regions around the centrilobular areas, which was consistent with biochemical results (Fig. 1C).

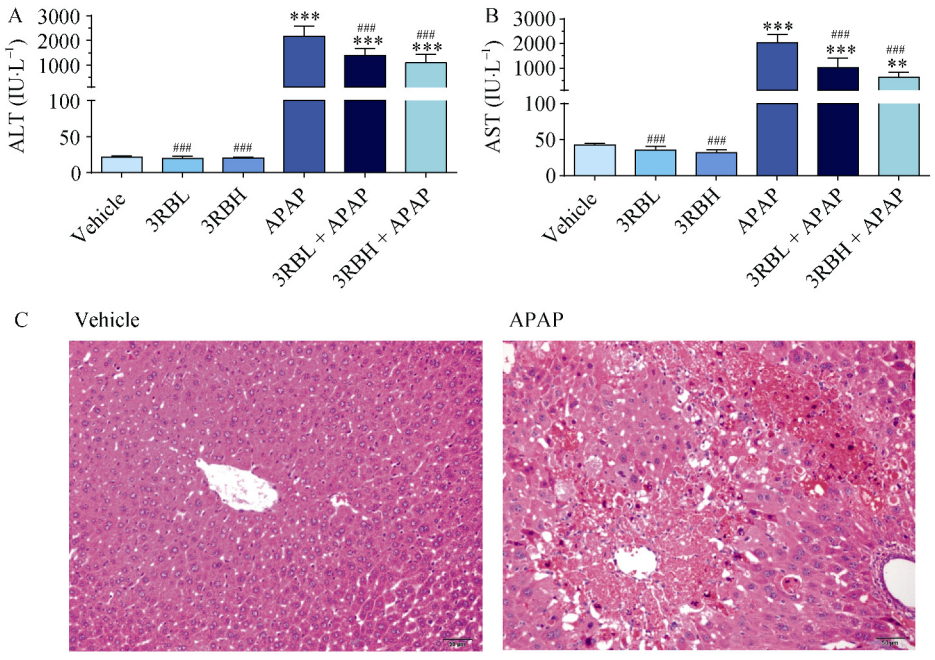

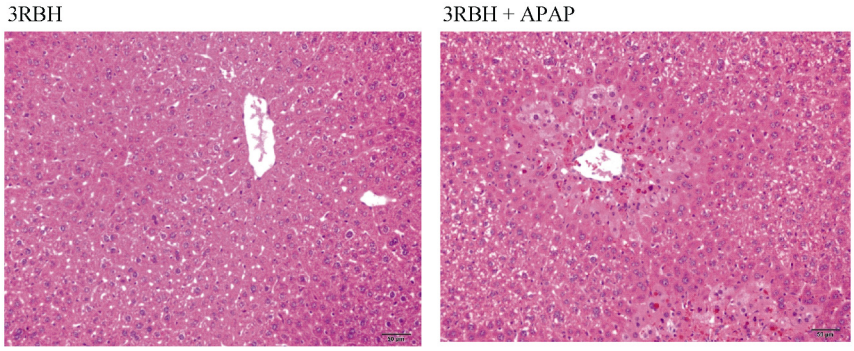

Fig. 1 Biochemical and histological study of the hepatoprotective properties of RB against APAP-induced ALI. RB was given to male ICR mice for 3 consecutive days prior to APAP administration. 6h after the third dose, APAP was given orally in a single dose (0.5 g·kg^{-1}), and all mice were sacrificed after 24 h. (A) Serum ALT levels. (B) Serum AST levels. (C) Representative H&E-stained liver sections（200 × magnification）in different groups. Vehicle, saline-treated mice; APAP, saline/APAP-treated mice; RBL or RBH, RB (9 or 36 g·kg^{-1})-treated mice; 3RBL + APAP or 3RBH + APAP, RB (9 or 36 g·kg^{-1})-treated for 3 continuous days and APAP- treated 6h after the third dose. Data are expressed as mean ± SD, n = 6. $^{**}P$ < 0.01, $^{***}P$ < 0.001 *vs* vehicle group; $^{###}P$ < 0.001 *vs* APAP group

LC-MS/MS results for toxicity-related biomarkers

The APAP toxic intermediate *N*-acetyl-p-benzoquinoneimine (NAPQI) is normally detoxified by conjugation with glutathione and subsequent hydrolysis into acetaminophen-cysteine (APC). Therefore, the pharmacokinetic parameters of the toxicity-related metabolite APC were determined using LC-MS/MS method. The plasma concentration-time profiles of APC in APAP group (1.2 g·kg^{-1}) with or without a 3-days RB pretreatment (6 or 25 g·kg^{-1}) in male Wistar rats are shown (Fig. 2A). Data was analyzed using Drug and Statistics software (DAS, Version 3.2, Wannan Medical College, Anhui, China) and improvements were found in the pharmacokinetic parameters profile. The $AUC_{(0\text{-}t)}$ decreased, and C_{max} reduced significantly (P < 0.05), which shows that accumulation of toxic product produced by excessive APAP were decreased accordingly (Figs. 2B and 2C).

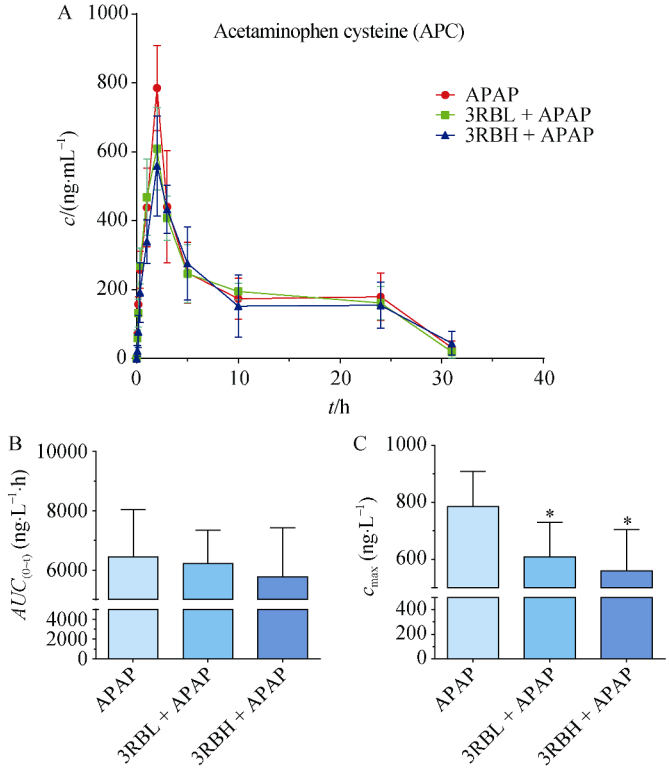

Fig. 2 (A) Plasma concentration-time profiles and (B, C) pharmacokinetic parameters profiles of APC in APAP (1.2 g·kg^{-1}) with or without a 3-days RB pretreatment in male Wistar rats. APAP, saline/APAP-treated rats; 3RBL + APAP or 3RBH + APAP, RB (6 or 25 g·kg^{-1})-treated for 3 continuous days and then APAP-treated in rats. Data are expressed as mean ± SD, n = 6. $^{*}P$ < 0.05 *vs* APAP group

LC-MS/MS analysis of cocktail probe substrates

After a three-day pre-administration of RB prior to APAP dosage, microsomes were prepared to conduct a cocktail approach. Five CYP probe substrate metabolites were determined using LC/MS/MS after incubation with hepatic microsomes. In our study, the levels of 6-CZX, 1-MDZ, and 5-OME in hepatic microsomes were significantly higher after APAP administration, suggesting that APAP can induce the activity of CYP2E1, CYP3A, and CYP2C in rats. Conversely, 6-CZX and 1-MDZ levels were significantly decreased after a high dose of RB combined with APAP, revealing inhibition of CYP2E1 and CYP3A activity.

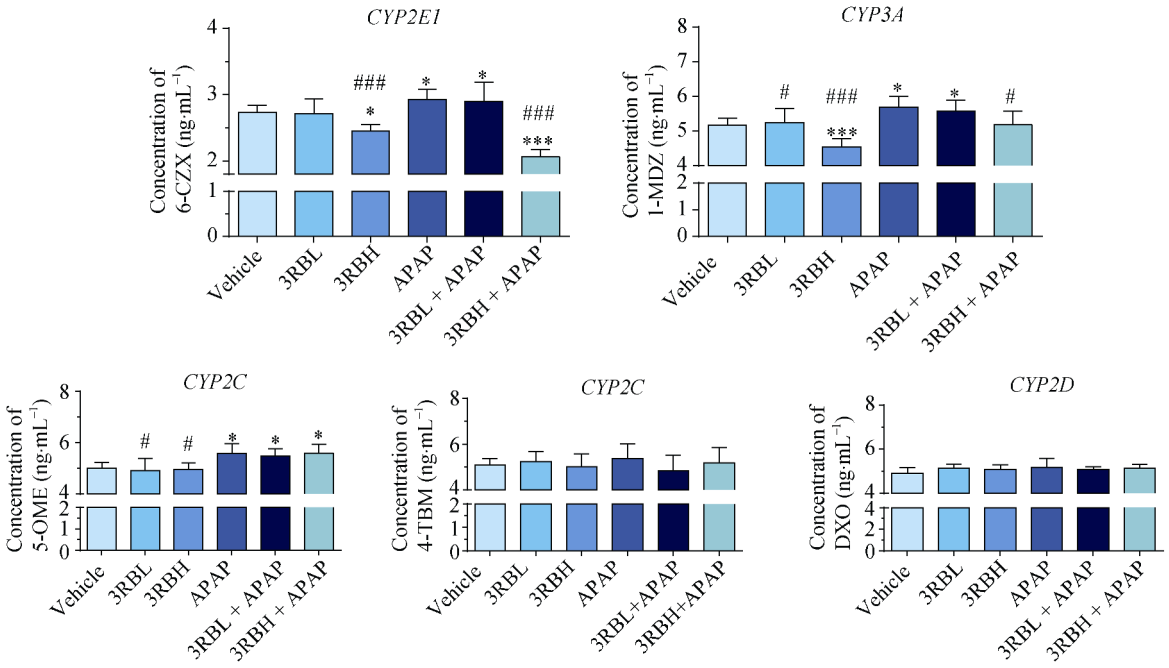

Fig. 3 The effect of RB on the activity of CYPs is measured *via* the concentrations of five CYP probe substrate metabolites in a cocktail approach. Vehicle, saline-treated rats; APAP, saline/APAP-treated rats; RBL or RBH, RB (9 or 36 g·kg^{-1})-treated rats; 3RBL + APAP or 3RBH + APAP, RB (9 or 36 g·kg^{-1})-treated for 3 continuous days and then APAP-treated in rats. Data are expressed as mean ± SD, n = 6. $^{*}P < 0.05$, $^{***}P < 0.001$ *vs* the vehicle group; $^{\#}P < 0.05$, $^{\#\#\#}P < 0.001$ *vs* the APAP group

Western blot and PCR analysis

To explore the changes in protein expression and gene expression levels of CYPs as well as to uncover the probable mechanism of the hepatoprotective effects of RB against APAP-induced liver injury, western blotting and PCR analysis were carried out. Compared to the APAP group, pre-administration of RB significantly reversed the increase in protein expression induced by APAP to an almost normal level, (especially the in CYP2E1and CYP3A), and had no significant effect on gene expression.

Conclusions

As the number of herbal remedies increased worldwide, regular users found that these natural remedies were not as nontoxic as they initially believed [22]. Therefore, many of them hesitated to use herbal medicines. Herbal medicines have been widely used for thousands of years due to its supposedly miraculous effect, especially in Asia [23]. However, processing and matching, dosage, and medication time were all crucial for effectiveness and avoiding toxicity.

RB has been used in traditional Chinese medicine (TCM) for over 2000 years [24], and with the development of TCM modernization, more and more RB preparations have been developed [25]. Despite its numerous pharmacological activities, we focused more on its side effects, especially potential in drug-drug interactions. Considering the combination use of APAP and preparations containing RB to treat colds, the safety of this combination is of great concern to us. Different ways of processing can produce different active chemical compositions, which can lead to opposite effects. To facilitate clinical use, aqueous extraction of RB was investigated here.

In the present study, the significant protective effects of RB against APAP-induced liver injury, as well as its underlying mechanism of action, were studied. Lower serum AST and ALT levels along with less liver damage were observed in mice when RB was pre-administered for three consecutive days before a toxic dose of APAP. A plasma concentration-time profile and pharmacokinetic parameters of the toxic related metabolite APC both revealed a lower exposure level and Peak Concentration in rats, suggesting that RB alleviated APAP-induced liver damage by prevented GSH depletion. Because APAP-induced hepatotoxicity is initiated by the excessive formation of NAPQI, and the metabolism of APAP is mediated by cytochrome P450, it was an important step to

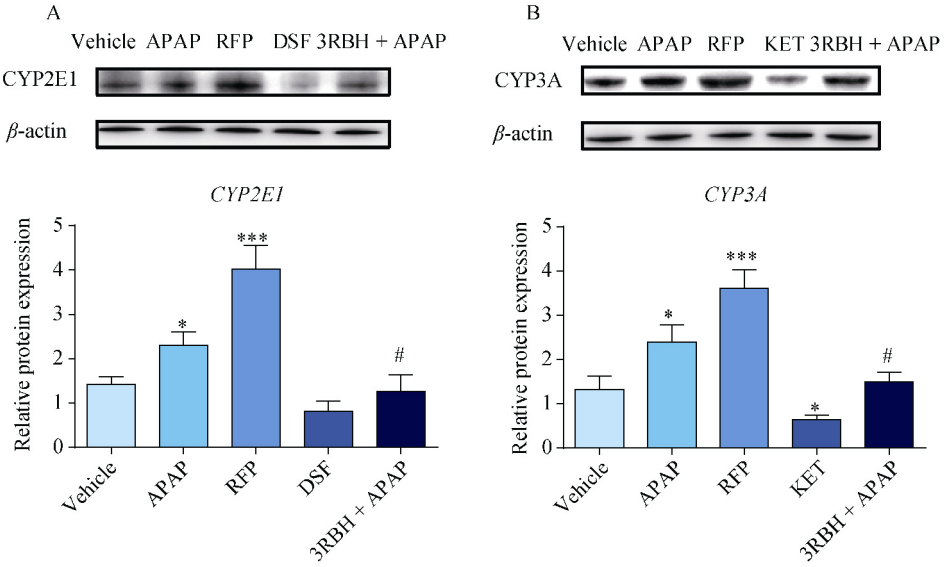

Fig. 4 The effect of RB on the protein expression levels of CYPs. Western blot results and densitometric analysis of CYP2E1 (A) and CYP3A (B) in livers from the vehicle group, the APAP (1.2 g·kg^{-1}) with or without a three-day pre-administration of RB (25 g·kg^{-1}) groups, the induced group (Rifampicin, 50 mg·kg^{-1}), and the inhibited group (Disulfiram 40 mg·kg^{-1} for CYP2E1, Ketoconazole 80 mg·kg^{-1} for CYP3A) in Wistar rats. Data are expressed as mean ± SD, n = 6. $^{*}P < 0.05$, $^{***}P < 0.001$ *vs* the vehicle group; $^{\#}P < 0.05$ *vs* the APAP group

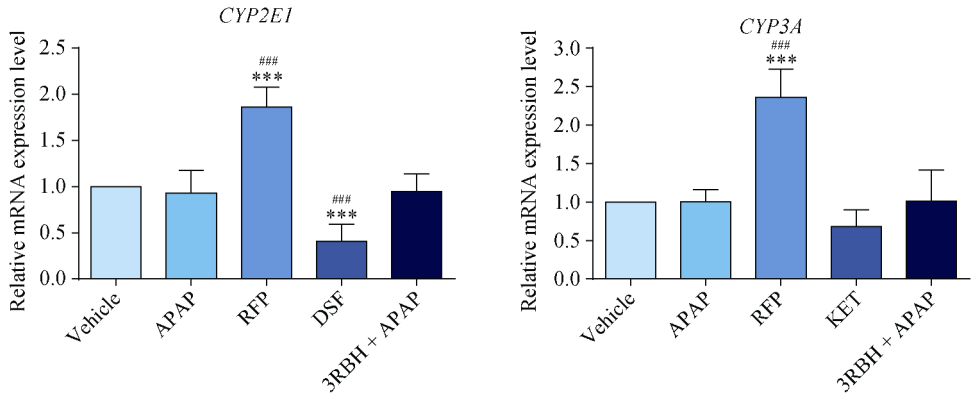

Fig. 5 The effect of RB on the gene expression levels of CYPs. Real-Time PCR results by comparative C_T($2^{-\Delta\Delta CT}$) method for CYP2E1 and CYP3A in livers from the vehicle group, the APAP (1.2 g·kg^{-1}) with or without a three days pre-administration of RB (25 g·kg^{-1}) groups, the induced group (Rifampicin, 50 mg·kg^{-1}), and the inhibited group (Disulfiram 40 mg·kg^{-1} for CYP2E1 , Ketoconazole 80 mg·kg^{-1} for CYP3A) in Wistar rats. Data are expressed as mean ± SD, n = 6. $^{***}P < 0.001$ *vs* vehicle group; $^{\#\#\#}P < 0.001$ *vs* the APAP group

identify the specific CYP isoforms involved in this case and to assess its inhibitive/inductive effect. The results of a cocktail approach showed significant inhibition of CYP2E1 and CYP3A activity when pre-administration of RB was coupled with APAP. Thus, it seems that the toxic metabolite NAPQI is derived from APAP and generated by CYP-catalyzed oxidation, mainly involving CYP2E1 and CYP3A reduction. Upon further investigation, RB significantly inhibited the protein expression of CYP2E1, CYP3A in rats, and had no significant effect on gene expression of these CYPs. It is therefore likely, that the changes observed in these enzymes expression mainly occurred in the translation process and not in the transcription of genes.

Overall, the findings of this study clearly demonstrated the hepato-protective effects of RB against acetaminophen-induced live injury *via* pretreatment. Although the mechanism of protection occurs partly through the inhibition of CYP450 activity, which mediates APAP metabolism, other signaling pathways and molecular mechanisms should be explored further. Moreover, the active compounds in RB should be screened for the potential candidates for the development of new hepatoprotective agents.

References

[1] *Pharmacopoeia of People's Republic of China*. Part 1 [M]. 2010: 263.

[2] Lizhi S. *Shennong's herbal* [M]. Shanghai Technology and Health Press, 1959.
[3] Wang C, Zhang T, Cui X, *et al*. Hepatoprotective effects of a chinese herbal formula, longyin decoction, on carbon-tetrachloride-induced liver injury in chickens [J]. *Evid Based Complement Alternat Med*, 2013, **2013**: 392743.
[4] Zhao W, Li JJ, Yue SQ, *et al*. Antioxidant activity and hepatoprotective effect of a polysaccharide from Bei Chaihu (*Bupleurum chinense* DC) [J]. *Carbohydr Polym*, 2012, **89**(2): 448-452.
[5] Di HY, Zhang YY, Chen DF. Isolation of an anti-complementary polysaccharide from the root of *Bupleurum chinense* and identification of its targets in complement activation cascade [J]. *Chin J Nat Med*, 2013, **11**(2): 177-184.
[6] Ashour ML. Ei-Readi M, Youns M, *et al*. Chemical composition and biological activity of the essential oil obtained from *Bupleurum marginatum* (Apiaceae) [J]. *J Pharm Pharmacol*, 2009, **61**(8): 1079-1087.
[7] Mohammadi A, Nazari H, Imani S, *et al*. Antifungal activities and chemical composition of some medicinal plants [J]. *J Mycol Med*, 2014, **24**(2): e1-8.
[8] Lee TF, Lin YL, Huang YT. Kaerophyllin inhibits hepatic stellate cell activation by apoptotic bodies from hepatocytes [J]. *Liver Int*, 2011, **31**(5): 618-629.
[9] Lee TF, Lin YL, Huang YT. Protective effects of kaerophyllin against liver fibrogenesis in rats [J]. *Eur J Clin Invest*, 2012, **42**(6): 607-616.
[10] Ou JP, Lin HY, Su KY, *et al*. Potential therapeutic role of Z-isochaihulactone in lung cancer through induction of apoptosis *via* notch signaling [J]. *Evid Based Complement Alternat Med*, 2012, **2012**: 809204.
[11] Yuan B. Yang R, Ma Y, *et al*. A systematic review of the active saikosaponins and extracts isolated from Radix Bupleuri and their applications [J]. *Pharm Biol*, 2017, **55**(1): 620-635.
[12] Mitka M. FDA asks physicians to stop prescribing high-dose acetaminophen products [J]. *JAMA*, 2014, **311**(6): 563.
[13] Blieden M, Paramore LC. Shah D, *et al*. A perspective on the epidemiology of acetaminophen exposure and toxicity in the United States [J]. *Expert Rev Clin Pharmacol*, 2014, **7**(3): 341-348.
[14] Bylda C, Thiele R, Kobold U, *et al*. Simultaneous quantification of acetaminophen and structurally related compounds in human serum and plasma [J]. *Drug Test Anal*, 2014, **6**(5): 451-460.
[15] McGill MR, Sharpe MR, Williams CD, *et al*. The mechanism underlying acetaminophen-induced hepatotoxicity in humans and mice involves mitochondrial damage and nuclear DNA fragmentation [J]. *J Clin Invest*, 2012, **122**(4): 1574-1583.
[16] Gonzalez FJ. The molecular biology of cytochrome P450s [J]. *Pharmacol Rev*, 1988. **40**(4): 243-288.
[17] Chen W, Koeniqs LL, Thompson SJ, *et al*. Oxidation of acetaminophen to its toxic quinone imine and nontoxic catechol metabolites by baculovirus-expressed and purified human cytochromes P450 2E1 and 2A6 [J]. *Chem Res Toxicol*, 1998, **11**(4): 295-301.
[18] Laine JE, Auriola S, Pasanen M, *et al*. Acetaminophen bioactivation by human cytochrome P450 enzymes and animal microsomes [J]. *Xenobiotica*, 2009, **39**(1): 11-21.
[19] Tonge RP, Kelly EJ, Bruschi SA, *et al*. Role of CYP1A2 in the hepatotoxicity of acetaminophen: investigations using Cyp1a2 null mice [J]. *Toxicol Appl Pharmacol*, 1998, **153**(1): 102-108.
[20] Schoel B, Welzel M, Kaufmann SHE. Quantification of protein in dilute and complex samples: modification of the bicinchoninic acid assay [J]. *J Bioche Biophys Methods*, 1995, **30**(2-3):199-206.
[21] Su T, Mao C, Yin F, *et al*. Effects of unprocessed versus vinegar-processed *Schisandra chinensis* on the activity and mRNA expression of CYP1A2, CYP2E1 and CYP3A4 enzymes in rats [J]. *J Ethnopharmacol*, 2013, **146**(3): 734-743.
[22] Lee CH, Wang JD, Chen PC. Risk of liver injury associated with Chinese herbal products containing radix bupleuri in 639, 779 patients with hepatitis B virus infection [J]. *PLoS One*, 2011, **6**(1): e16064.
[23] Zhang L, Schuppan D. Traditional Chinese Medicine (TCM) for fibrotic liver disease: hope and hype [J]. *J Hepatol*, 2014, **61**(1): 166-168.
[24] Xie H, Huo KK, Chao Z, *et al*. Identification of crude drugs from Chinese medicinal plants of the genus Bupleurum using ribosomal DNA ITS sequences [J]. *Planta Med*, 2009, **75**(1): 89-93.
[25] Li C, Liu Y, Liu Y, *et al*. Advances in research of chemical constituents and active constituents of *Bupleurum chinense* DC. [J]. *Chin Arch Tradit Chin Med*, 2014, **32**: 2674-2677.

Cite this article as: WANG Yu-Xin, DU Yi, LIU Xia-Fei, YANG Fang-Xiu, WU Xiao, TAN Li, LU Yi-Hong, ZHANG Jing-Wei, ZHOU Fang, WANG Guang-Ji. A hepatoprotection study of Radix Bupleuri on acetaminophen-induced liver injury based on CYP450 inhibition [J]. *Chin J Nat Med*, 2019, **17**(7): 517-524.